IAC-04-IAF-Q.1.01

COROT MISSION ENGINEERING : COST-EFFECTIVE SOLUTIONS FOR STELLAR PHOTOMETRY IN LOW EARTH ORBIT

L. BOISNARD, COROT System Engineer
Centre National d'Etudes Spatiales, Toulouse, France
laurent.boisnard@cnes.fr

M. AUVERGNE, COROT Project Scientist
Observatoire de Paris, LESIA-CNRS UMR 8109, Meudon, France
michel.auvergne@obspm.fr

ABSTRACT

The COROT space telescope is an experiment of astronomy dedicated to stellar seismology and search for extrasolar planets. The mission is led by CNES in association with French laboratories and with a significant international participation: ESA, Austria, Belgium, Germany contribute to the payload, whereas Spain and Brazil, which has recently joined the project, both contribute to the ground segment. Based on a PROTEUS low earth orbit recurrent platform, the spacecraft has been in development since October 2000 for a launch scheduled in July 2006. Taking benefit of the conclusions of several project reviews held recently, this paper represents the work of the COROT team. It gives an overview of the experiment, explains where the critical scientific requirements are for payload engineering and describes the cost-effective compromises found for high accuracy photometry in low earth orbit. We run through the different families of perturbations due to the interaction between the spacecraft and its environment and illustrate how some noise contributors, which generate spectral lines likely to be misinterpreted as a component of the star signal, are reduced by design, avoided by an appropriate mission profile or corrected after calibration. We focus on the following technical issues: telescope baffling and orbital drift, pointing stability, optoelectronics thermal regulation, light curve processing.

1. THE COROT MISSION

1.1. The scientific objectives

The COROT mission has two scientific programs, both requiring long uninterrupted observations with very high photometric accuracy. They work simultaneously on adjacent regions of the sky.

1.1.1. Stellar seismology

A star is a mass of hot gas, subject to forces of gravity, pressure and Coriolis inertia when it rotates. These forces play like the spring forces of an oscillator with quantified eigenmodes. The stationary waves associated with these hydrodynamic processes make the surface distort and are the source of photon flux oscillations, whose amplitude is expected to be about a few 10^{-6} (ppm). Inside a star, the waves propagate at a sound speed proportional to $T^{1/2}$ (T is the gas temperature), following a path whose maximum depth depends on the wave frequency. Therefore, the seismology spectrum of a star is likely to reveal some important parameters of its internal structure. For example, the analysis of a seismology spectrum make it possible to estimate the density across a region of acoustic stationary modes, the chemical composition near the stellar core or the distance at which convective heat transport becomes preponderant over radiative heat exchanges. Applied to the Sun, the helioseismology has proved to be a powerful tool to probe its interior, leading to identify many parameters of solar physics with an accuracy better than 0.1% down to the core, and even contributing to rethink the theory of the neutrinos.

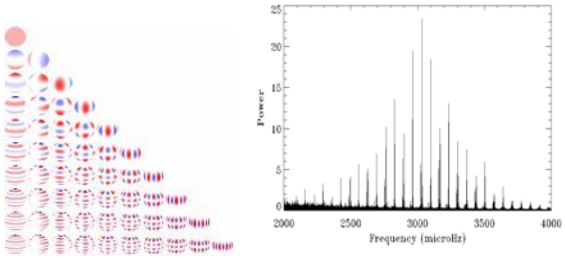

Fig.1: Left: example of surface spherical harmonics (of degree l from 0 to 9 and of azimuthal order m from 0 to l). Right: solar spectrum measured by VIRGO.

Now, the observation from space of other stars (with a precision and over time scales out of reach from the ground) is very much needed to test different physical conditions and improve the modeling of intermediate mass stars.

Long runs (central program)

Focused on the internal hydrodynamic processes of stars in the main sequence evolution stage and around it, the seismology central program will study in details the variations (down to 10^{-6}) of the luminous flux emitted by a small number (50) of stars brighter than magnitude 9. The associated observing runs last 150 days, which provides a resolution of 0.1 μHz in the Fourier space. This frequency resolution is necessary to discriminate a significant number of modes, to reveal the frequency splittings and to rebuild the line profiles.

Observing run duration	150 days
Number of targets	10
Magnitude of targets	brighter than mv=9 main target at mv=6
Number of runs	5
Total number of targets	50
Families of targets	solar type stars (F,G) δ Scuti, γ Dor (A, F)

Table 1: Main features of long observing runs.

Although a space telescope like COROT cannot produce a surface cartography of the oscillating modes on distant objects, the light curve integrated over the stellar disk will bring accurate information on the radial modes and make it possible to determine:

- the radius of the core (where thermonuclear reactions take place),
- the Helium content,
- the deep limits of the convective external layers,
- the profile of the rotation velocity from the center to the surface of the star,
- the associated angular momentum transport.

Seismology measurements will be performed in the following bandwidth: [0.1 ;10] mHz, covering both pressure modes of stars of spectral types F and G (higher frequencies) and gravity modes of stars of spectral type A (lower frequencies). Gravity modes, not detected on the Sun, could be observed in stars where the associated excitation mechanism is strong enough in the H or He ionization layer and where there is no external convective layer to damp them.

The main target stars are typically F, G or δ Scuti (A) stars with a magnitude less than 6.5. As a result of scientific arbitration, other types of target stars have been selected such as γ Dor or β Ceph. These stars are known for high amplitude oscillations, detected from the ground. But these modes are supposed to be a small number among many other modes of low amplitude. In the vicinity of a main target, some additional stars, brighter than a magnitude 9 and belonging to an extended range of stellar types (peculiar metallic stars, sub-dwarfs of B type, Be stars, …), will also be studied. COROT is designed to acquire up to 10 stars simultaneously.

Short runs (exploratory and additional programs)

The purpose of the exploratory program is to observe a wide variety of stars (from B to K spectral types) up to magnitude 9, where the Hertzsprung & Russel (HR) diagram is scanned.

This will be accomplished by inserting a 20-day observing run between two long runs of the central program. With this shorter time window, the resolution on the frequencies falls to 0.6 μHz, but it is sufficient to produce statistical data about the excitation of the oscillating modes, as a function of mass, age, rotation speed and metallicity.

Observing run duration	20-30 days
Number of targets	10
Magnitude of targets	brighter than mv=9
Number of runs	5-10
Total number of targets	50-100
Families of targets	many types across the HR diagram

Table 2: Main features of short observing runs.

Open to additional astrophysical programs, the COROT mission will also allow some astronomers' communities to propose short runs devoted to specific target fields. The light curves thus collected may be interesting in domains such as stellar activity (surface magnetism), tides in binary systems, pulsating stars beyond the instability strip, search for Kuiper belts objets, etc.

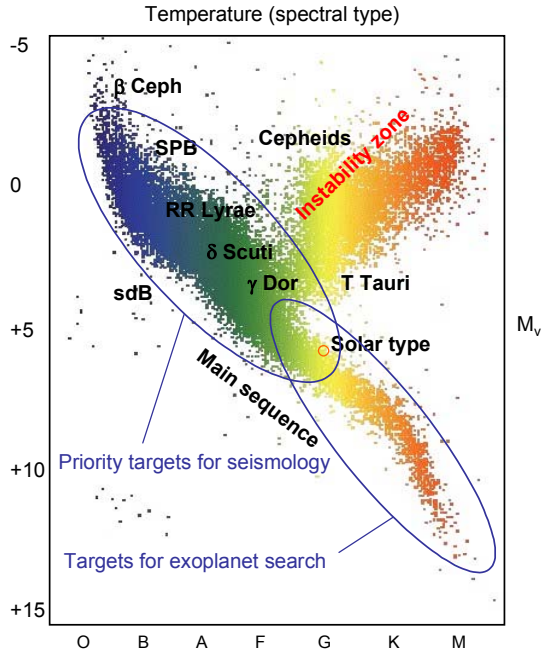

Fig. 2: Priority families of targets observed by COROT in the HR diagram.

1.1.2. Search for extrasolar planets

The COROT planet-finding program aims at detecting the presence of extrasolar planets when they transit in front of their parent star. By adapting both the integration time and the focus conditions on the exoplanet channel, but without any major change in the experiment design, luminous flux variations down to 7.10^{-4} (ground integration time : 1 hour) can be seen by COROT in a large variety of stars whose magnitude ranges between 12 and 15.5. That is compatible with the small luminosity decrease of a star occulted by a planet slightly bigger than the Earth (twice the Earth radius). After the discovery of giant planets by the radial velocity method, COROT should detect the first terrestrial planets (out of reach from the ground).

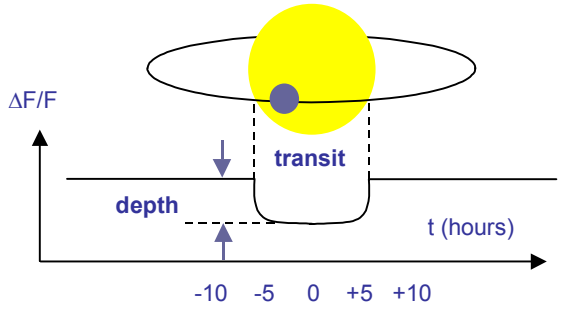

Fig.3: Principle of detection of a planetary transit.

Parameter	Equation	Hot Jupiter	Earth like
Detection probability (p)	R_s / a	5%	0.5%
Depth of signal ($\Delta F/F$)	$(R_p / R_s)^2$	10^{-2}	10^{-4}
Transit duration (tr)	(P/π) (R_s/a)	3 h	11 h

R_p is the radius of the planet
R_s is the radius of the parent star
a is the orbit radius (orbit supposed to be circular)
P is the orbit period of the planet

Table 3: Parameters of a planetary transit.

To detect a planet with complete confidence, the phase must stay coherent over 3 observed periodic transits. Given the 150-day observing runs imposed by the seismology central program, the longest period for planetary transits is 50 days. In order to partly overcome this limitation, a dispersion device has been placed in front of the exoplanet CCD matrices, providing a three-color signal which helps to make the difference between planetary transits (achromatic events) and stellar activity (highly chromatic due to temperature variations at the surface of the star). Studies show that the use of this colored information improves the detection with stars much more active than the Sun and will contribute to widen the detection domain to cases where a run is not long enough to show three periods. One gets a better confidence for mono-transits, interesting in particular for Jupiter-like or Uranus-like planets, whose depth of signal is reachable (as one can see in table 3, the depth of the signal is independant of a).

Observing run duration	same as for seismology
Number of targets	12 000
Magnitude of targets	$12 \leq mv \leq 15.5$
Number of runs	same as for seismology
Total number of targets	up to 180 000
Families of targets	red dwarfs, F to M

Table 4: Main features of observing runs.

In addition to hundreds of hot Jupiters (easy to detect by occultation), between 10 and 40 terrestrial planets should be detected, some of them in the "habitable zone" (temperature compatible with liquid water), depending on hypotheses about accretion models and planets' existence. It must be mentioned that the detection of planetary bodies in the habitable zone is most likely to occur round cold dwarfs of M type (habitable zone closer to the parent star, between 0.2 and 0.5 a.u).

1.2. The COROT satellite

The COROT spacecraft is based on a PROTEUS low earth orbit recurrent platform, developed by CNES and Alcatel Space.

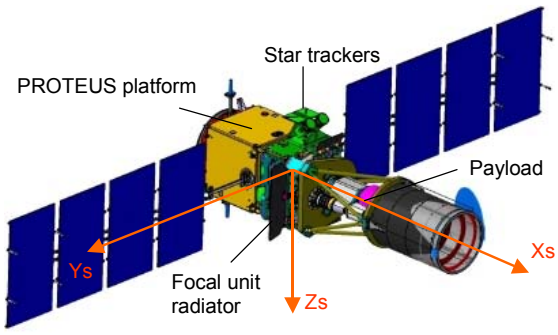

Fig. 4 : Satellite overview (4.20 m x 9.60 m)

This platform was used for the first time by the French-US oceanography JASON satellite, launched in 2001. In the configuration adopted by COROT, several sub-systems have been upgraded : Li-Ion battery, high capacity magneto torquer bars, new star trackers (SED-16).

The satellite will be operated from the COROT Control Center, located in Toulouse and sharing the facilities of the PROTEUS satellites family. The preparation of the observation sequences and the pre-processing of the scientific data will be done by the COROT Mission Center, located in Toulouse and having interfaces with the laboratories. A network of automatic S band

ground stations (Kiruna, Aussaguel, Natal) will be used for communication with the satellite. It will offer up to 6 visibilities per day. The volume of data to be transmitted daily to the ground is 1.4 Gbits.

The COROT payload is made up of the following sub-systems :

- Corotel : an afocal telescope (pupil of 270 mm) composed of 2 parabolic mirrors, with a cylindrical baffle to stop the Earth straylight and a one-shot cover against blinding in early attitude acquisition phase.
- Corotcam : a wide-field camera composed of a dioptric objective (6 lenses) and a focal unit equipped with 4 frame transfer CCD 2048 x 4096. A dispersive device (bi-prism) is inserted in front of the two CCD matrices dedicated to exoplanets.
- Corotcase : the equipment bay supporting scientific data processing electronics (video electronics, extraction units and data processing units) and instrument housekeeping electronics (power distribution, fine thermal control, calibration management, synchronization unit).

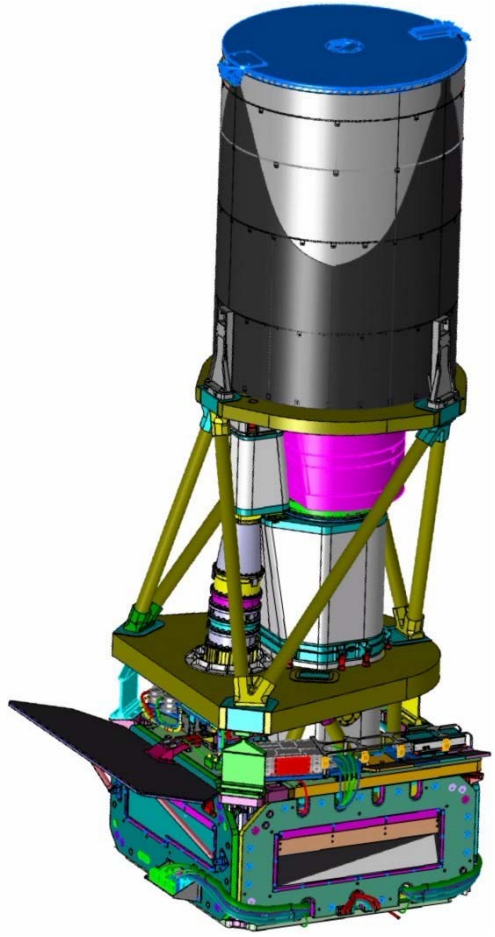

Fig. 5: Payload overview (equipment bay in the lower part, camera and telescope in the upper part).

The main characteristics and performances of the spacecraft are summarized hereafter :

Mass	Bus dry mass = 270 kg Propellant mass = 30 kg Payload mass = 300 kg
Length	4.20 m
Diameter	2.00 m (under fairing)
Power	Bus consumption = 300 W Payload consumption class = 200 W 2 symmetric wing arrays Li-Ion battery
AOCS	Gyro-stellar unit with 2 star trackers and 3 2-axis gyrometers Magnetometers and sun sensors 4 reaction wheels, desaturated by magneto torquer bars (MTB) 4 1N thrusters for orbit maneuvers
ΔV capacity	90 m/s for 600 kg (hydrazine)
Pointing	0.05° (3σ) on each axis Improved to 0.5 arcsec for COROT
Datation	Derived from a GPS receiver Compatible with 10^{-6} accuracy
Data handling	Centralized architecture 2 MA 31750 Processors MIL-STD-1553 bus Discrete point to point lines
Data storage	2 Gbits (mass memory)
Links	S band QPSK CCSDS packet standard protocol TM frames data rate = 735 kbits/s TC frames data rate = 4 kbits/s

Table 5: Technical characteristics of the spacecraft.

1.3. Orbit, flight domain and mission profile

As COROT flies on a PROTEUS bus, only low earth orbits are allowed. In order to observe the same direction of the sky for a long period of time (several months), not being blinded by the Sun or occulted by the Earth, the satellite must have a polar inertial orbit and a line of sight roughly perpendicular to the orbit plane. The orbit parameters are listed hereafter:

Semi-major axis (a)	7274 km (altitude 896 km)
Eccentricity (e)	0.00127° (circular)
Inclination (i)	90°
Right Ascension of Ascending Node (Ω)	12.5° (or 192.5°)
Period (T)	6174 s (1 h 43 min)
Local time variation	-4 min/day

Table 6: Orbit parameters and associated properties.

Once given the orbital movement, the constraints to be taken into account for the orientation of the spacecraft are:

- Sun glare: the observations are possible when the direction of the Sun is at more than 90° of the observed field.
- Straylight scattered by the Earth: at the altitude of 896 km, the Earth is still seen as a big sphere and the limb is a source of scattered light. Considering that the line of sight must remain at more than θ =20° from the limb (limit of baffle efficiency), the radius of the observation cone is γ = acos (R/a) - θ = 10° (see fig. 6).
- Roll domain: $\pm$ 20° on the boresight axis, after alignment of the solar arrays for the optimum power budget. Such a rotation is helpful to optimize the projection of the target stars onto the CCD matrices (to put targets out from saturated columns, for instance).

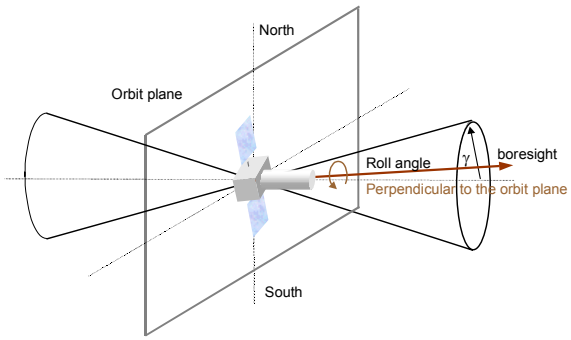

Fig. 6: Limits of the flight domain (inertial orbit).

- Payload thermal constraints: because of the focal unit radiator, the Ys+ satellite wall must be in the shade as much as possible (northward in winter, southward in summer). Ys+ will be exposed to the Sun only when the Earth is close to the Line of Equinoxes (low solar declination, high solar azimuth in the radiator reference frame).

It must be mentioned that the upgrade of the PROTEUS electrical chain, consisting in replacing the Ni-Cd battery by a Li-Ion battery with a lower thermal dissipation, has led to remove any constraint on the bus sidewalls. The battery sidewall can withstand any solar incidence. The rotation of the solar panels is performed every 14 days.

Taken together, these constraints lead to a set a rules which determine the mission scenario, with two reversal maneuvers per year, when the direction of the Sun is perpendicular to the line of sight. Each half year period contains a long run and one or two short runs. As a function of the right ascension of the depointing, the reversal maneuvers will be performed close to the line of nodes in a range of 20 days.

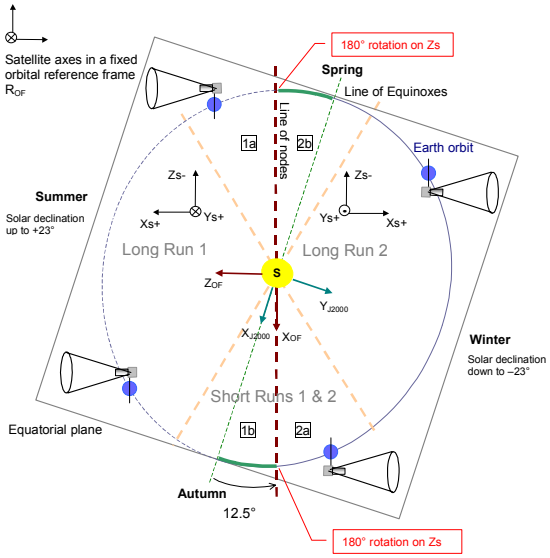

Fig. 7: Mission profile and attitude maneuvers.

Ω determines the direction of the orbit plane, therefore the direction of the observation cone. The optimized value Ω=12.5° (defined by the scientific committee on the basis of preparatory observations) has been chosen in order to look at a dense region of the sky where the galactic plane intersects the equatorial plane (see Fig. 8).

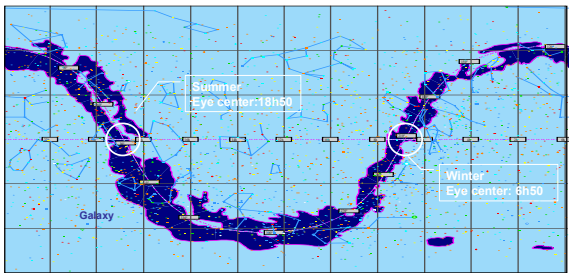

Fig. 8: The sky observed by COROT.

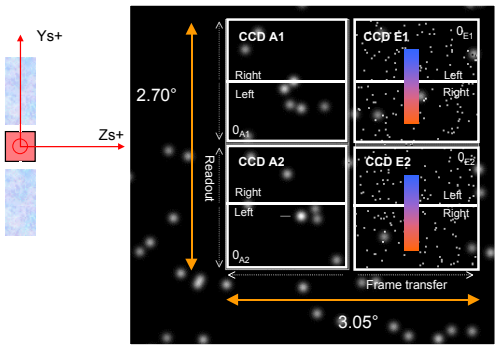

Fig. 9: Field of view for seismology and exoplanets. Direction of dispersion is indicated by color bands.

The field of view is 2.7° x 3.05°. The relative position (left/right) of seismology and exoplanet channels has been defined at the same time as the orbit plane, as a compromise between the two programs to set each half-field in the most favorable orientation inside the observed sky.

The characteristics of the sky in the eyes, centered at 6 h 50 (winter) and 18 h 50 (summer), are:

- At least 10 main target stars meeting the criteria of magnitude and spectral type for the central program. It has been verified by high angular resolution imagery that these stars are not polluted by faint stars at less than 60 arcsec.
- More than 800 stars as secondary targets, brighter than magnitude 8 (excluding the giant ones). Photometric and spectroscopic ground based observations are in progress to measure their fundamental parameters: mass, temperature, metallicity and rotation velocity.
- A density of red dwarfs higher than 1500 per square degree (magnitude less than 15.5) for the exoplanet program.

1.4. Duty cycle

Every interruption in the data makes the signal-to-noise decrease and affects the seismology spectrum by windowing. The mission scenario and the sensitivity of the equipment to radiations must guarantee continuous observations as much as possible. When increasing, a perturbation can be considered as a cause of unavailability.

The estimated values are 97% over 5 moving days for seismology and 88% over a long run for exoplanets. Periodic crossings of the South Atlantic Anomaly turn to be the main contributor.

2. PERFORMANCES AND DESIGN

2.1. Photometric performances

2.1.1. Seismology channel

For stochastically excited modes, the accuracy one can get on the position of a spectral line is a function of the observing run duration, the oscillating mode lifetime and the signal-to-noise ratio. Expected to have mode lifetimes of about 5 days, the target stars must be observed for 150 days with a minimum signal-to-noise ratio of 16 (in terms of power spectral density). See reference (1) for more details.

Random noise

With the objective to detect 2.5-ppm oscillations for G-type stars over their expected mode lifetime, the photon noise level in the Fourier spectrum is required at 0.6 ppm and determines the efficiency of the instrument at the magnitude 5.7 : n=6 10^6 electrons/s. The standard deviation of the photon noise is about 2500 electrons/s.

The latest assessments of the instrument efficiency made at the payload Critical Design Review (CDR) lead to: n=7.3 10^6 electrons/s with a photon noise of 2700 electrons/s in beginning of life. The level of signal-to-noise ratio is thus expected good.

The objective is to keep every other source of random noise below 1/10 of this reference noise. The main performances required and expected are given below:

Straylight	< 15 photons/pixel/s Including the zodiacal light
Jitter noise	< 0.5 arcsec (probably less than 0.3 arcsec) uniformity of the detectors better than 1%
CCD readout and electronics noise	< 14 electrons rms/pixel/s (measured at 8 electrons rms))
Thermal sources	
Defocus	< 10 μm 0-peak (estimated at 0.5 μm)
CCD thermal variations	< ± 0.015° C peak-peak (estimated at ± 0.006° C)
CCD efficiency sensitivity	< 5 10^{-3} /° C (measured at 10^{-3} /°C)
Video electronics thermal variations	< ± 0.15° C peak-peak (estimated at ± 0.07° C)
Video electronics gain sensitivity	< 0.1 10^{-3} /° C (measured at 0.02 10^{-3} /° C)
Note : the image spot of a 5.7 magnitude star stretches over 410 pixels, the integration time is 1s.	

Table 7: List and level of the principal noise sources.

As a result of this budget, the noise level in the Fourier spectrum is expected close to :

- 0.56 ppm for a magnitude 5.7,
- 2.7 ppm for a magnitude 9.

Structured noise and periodic perturbations

Seismology will be performed in the following bandwidth : [0.1 ; 10] mHz. Every structured noise having spectral lines between 1 minute and 3 hours is likely to hide a number of components of the star signal. The orbit period (frequency of 0.16 mHz) and its first harmonics are in the low frequency part of the band. It has been necessary to make the inventory of the possible periodic perturbations and to reduce them by design, by the mission profile or by calibration.

In order to avoid the on-board implementation of expensive technologies and considering that gravity modes should be less numerous than pressure modes, it has been accepted to pollute 10% of the low frequency domain, which represents 100 μHz in the interval of [0.1 ; 1] mHz.

There is pollution when, in the Fourier spectrum, a lobe of a sine perturbation is higher than the photon noise. Analytically, for a series of perturbations at the frequencies f_i with the amplitude A_i and the coherence time Q_i, one can write the following formula:

$$\sum_i 2A_i / (\pi b_{phot}(T)) 1 / Q_i < 100 \mu Hz \quad (1)$$

The first factor is the number of lobes of the perturbation i higher than the photon noise (function of the run duration T) and the second one is the width of a lobe. This criterion is used to manage the noise budget at system level:

Straylight Ecartometry Thermal variation of opto-electronics	1 line at 10 ppm (coherent) 0.16 mHz	25 μHz
Gravity gradient ACS harmonics	5 lines at 2 ppm (coherent) [0.1 ; 0.5] mHz	25 μHz
ACS harmonics Albedo variations	5 lines at 0.2 ppm (non coherent) [0.5 ; 1.0] mHz	< 50 μHz
Note: Q_i = 0.5 μHz for a coherent perturbation Q_i = 10 μHz for a non-coherent perturbation		

Table 8: Budget of pollution in the Fourier spectrum.

At instrument level, every source of periodic noise shall be kept at 50 ppm. The sensitive equipment will be characterized before the launch and a set of temperature probes will be mounted on the payload for subsequent light curve corrections, compatible with a performance of 2 ppm.

For example, the instrument is designed to have a CCD temperature peak stability about 0.015° associated with a knowledge of the temperature curve itself better than 0.005°. The knowledge of every thermal stability coefficient (CCD efficiency, electronics gains, offsets) is estimated at 1%.

2.1.2. Extrasolar planet channel

Given the efficiency of the telescope and the typical image parameters for the exoplanet channel :

- elementary integration time : 32 s,
- PSF over 25 pixels for a reference K0 star,
- optical transmission of the prism : 0.9,

the flux at the magnitude 15.5 is : n=1200 electrons/s. The standard deviation of the photon noise is about 35 electrons/s.

The requirement to detect a change of stellar flux equal to 7 10^{-4} (integrated over 1 hour) for a 15.5 magnitude K0 star is fulfilled if the global random noise is twice the photon noise.

According to recent estimates, the random noise budget is 1.8 times the photon noise. Moreover, a change of stellar flux of 1.2 10^{-3} is detectable in the blue color at mv=15.

Concerning the periodic perturbations, because of the windowing of the CCD (see chapter 3), the exoplanets program asks for an additional requirement of optical distortion stability : 0.05% over the orbital period.

2.2. Strategy for critical noise contributors

For each source of noise identified above, the strategy is quickly described.

2.2.1. Straylight

With a circular orbit at 896 km, the main difficulty is to protect the photometer against the straylight coming from the Earth. At 20° from the limb, the collected flux is around 10^{20} photons/s. To reach a residual flux of 1 photon/pixel/s at focal plane level, the instrument shall have a 10^{-13} rejection coefficient, which is the highest capacity ever required for a telescope of this class.

Other solutions being excluded for insufficient straylight rejection capacity, a telescope with 2 co-focal parabolic mirrors has been the concept adopted.

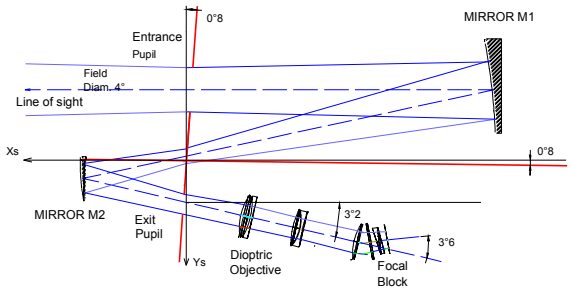

Fig. 10: Telescope concept (afocal and camera).

The focal plane of the two mirrors is shared by the entrance and exit pupils, and by a square field stop. The elliptical entrance pupil of equivalent diameter 270 mm is reduced by a factor 3. The 6-lens dioptric camera is placed in the collimated exit beam. The focal length is 1.2 m. The purpose of the dioptric objective is to correct a number of aberrations introduced by the afocal part, mainly field curvature and coma. Thus we can reach a good level of uniformity of the image spots across the field of view.

The capacity of rejection, associated with the weight (24 kg) and volume allocations, needs a high-performance compact baffle to be achieved.

The external baffle is a delivery of the CSL (Centre Spatial de Liège), with Verhaert as manufacturer. The internal baffle, made up of two parts protecting respectively the two cavities between the entrance pupil and M1 and between M2 and the exit pupil, completes the set of the telescope components

against lateral and rear straylight (coming from the Sun). Mechanical vanes and opaque flexible joints guarantee no straylight at the interfaces. The internal devices are developped by Alcatel Space, also in charge of the telescope integration.

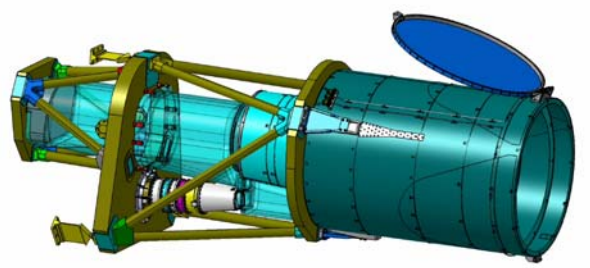

Fig. 11: CAD-view of the telescope, with external and internal baffles. The mirror M1 is partly protected by the equipment bay.

The main characteristics relative to straylight rejection are the following :

Length	2700 mm (2 stages)
	1660 mm (external part)
Entrance diameter	840 mm
Contamination level	2000 ppm in orbit
Internal design	Low diffraction chicanes (10) against grazing incidence reflections
Mirror roughness	< 1 nm
	(to prevent third diffusion)
Coating	black paint (albedo <4%)

Table 9: Main characteristics of the baffling system.

The efficiency of the baffle to stop the rays at different incidence angles has been calculated and, with a modeling of the Earth albedo, the flux of straylight seen by the detector has been estimated. This study has shown that the scattered light is seen by COROT as a periodical function with a maximum amplitude when the satellite flies over the day part of the Earth (see the graph below). Polar caps contribute, but are not predominant.

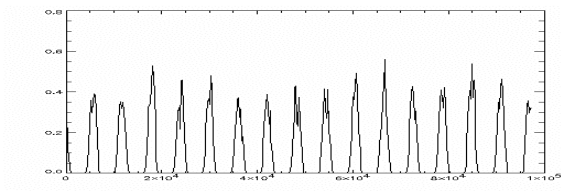

Fig. 12: Orbital variations of straylight intensity over 15 orbits (beginning of a half year period).

The maximum intensity depends on the date and is highly influenced by the direction of observation at the beginning or at the end of a half year period. The graph below shows it will not be possible to stay under a few photons/pixel/s during a long run if the depointing is higher than 7°. The level of straylight rockets to 100 photons/pixel/s between 7° and 12°. As polar caps contribute less than day part of the Earth, the curves are less sensitive to declination than to right ascension. The minimum of staylight is reached close to the solstice, when the Sun is in the back of the satellite.

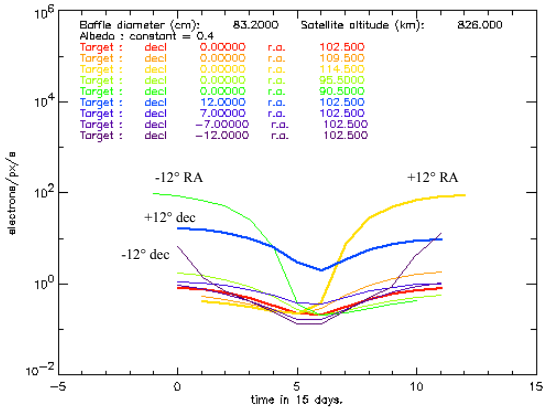

Fig. 13: Maximum straylight over 6 months. Set of plots for different directions of the line of sight. The depointing angle from the eye center ranges from -12° to +12° both in right ascension and declination.

Drift of the orbit

A solution to observe the targets of the seismology central program and the associated exoplanet fields in a configuration as close as possible to the eye center, is to make the orbit plane drift. A maneuver to change inclination can start or stop the drift, whose speed is given by :

$$d\Omega / dt = \frac{3}{2} J_2 a_e^2 \sqrt{\mu} \frac{\Delta i}{a^{7/2}} \qquad (2)$$

For example, if $\Delta i = -0.1°$, $d\Omega/dt = -4°$/year.
The cost in increment of speed ΔV is 13 m/s. 26 m/s can be reserved for such operations. Thrusters being along Xs, no specific attitude maneuver of the spacecraft has to be performed (the operation is done just before or just after a reversal maneuver and takes a week by performing a series of small ΔV).

A proposal submitted to the scientific committee consists in changing the initial value of Ω and start a drift after a year of mission. The graph below shows that the eye moves along the Equator in such a way that every main target can be observed (in the order of the decreasing right ascensions) at less than 7° from the center, where the performance of straylight is expected good.

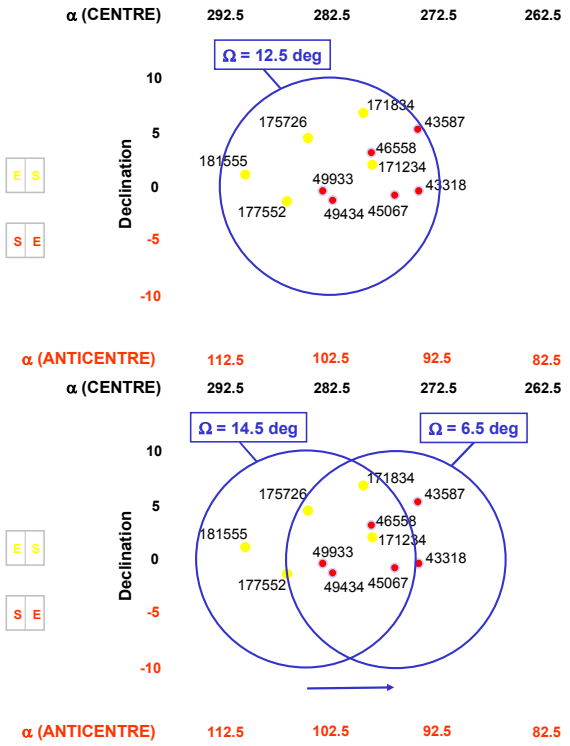

Fig. 14: Movement of the eye along the Equator (drift of -4°/year over a period of two years).

2.2.2. Pointing and AOCS

A movement of the spot on the CCD surface changes the integrated photometry because the set of impacted pixels is not the same. The associated noise is proportional to the pixel response non uniformity (σ_{PRNU}) and to the amplitude of the random movement (dx). It decreases with the diameter (D) of the spot.

$$\sigma / N \propto \sigma_{PRNU} dx / D^{3/2} \quad (3)$$

To comply with a coupled photometry/jitter noise 10 times lower than the photon noise ($\sigma/N < 4.10^{-5}$), the satellite pointing stability requirement is stringent: 0.5 arcsec rms, implying the use of the instrument for ecartometry. The periodic and random noises due to the sensor are divided by 10 while thermo-elastic biases between star tracker and payload frames are removed.

The AOCS loop has been modified and a specific mission mode is implemented in the PROTEUS on-board software. The usual kinematic filter has been replaced by a dynamic kalman filter. Two target stars of the seismology program will be used by the ecartometric algorithm, to be performed at payload level (inversion of a jacobian matrix built from the movement of the target stars' barycenters). To avoid angular periodic errors due to the focal length thermal variations, the focal length is estimated in real time. Small gaps of perturbations should remain during eclipse entries/exits and solar panel rotations. In the same way, the performance of the barycenter measurements should be altered when the satellite crosses the South Atlantic Anomaly. But new Magneto Torquer Bars (MTB), with a higher capacity (180 $A.m^2$) and driven by a proportional control law, make it possible to remove the orbital noise usually associated to the periodic desaturation of the reaction wheels.

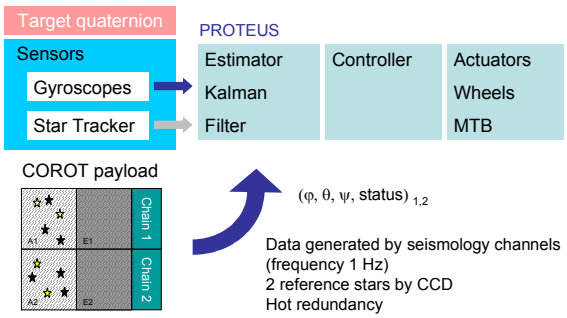

Fig. 15: Architecture of the ACS (hybridization of gyroscope data with payload ecartometry).

The transition from the PROTEUS standard mode to the mission mode is performed in two steps:

- The first step uses the star tracker data, while the instrument data are processed in parallel in another attitude estimator. The size of the star windows is adapted to the thermo-elastic drift between the payload and the gyro-stellar unit reference frames over the useful segment of the orbit (star tracker's field of view not masked by the Earth). A comparison of both attitude estimators convergence is made on the ground, before switching to the instrument data.
- The instrument data are used to drive the control loop, before a second transition to program a change in the acquisition windows of the CCD (size, binning). From then on, the CCD sequencers of the seismology channels are in configuration to perform the scientific on-board treatments.

The main results of a series of simulation runs where the instrument is driving the AOCS loop are given in table 9 and in graph 16.

Satellite axis	Xs	Ys	Zs
Noise in arcsec	1.44 *(24)*	0.19 *(0.3)*	0.27 *(0.3)*

Table 10: Random noise estimate for each satellite axis (the specification is given between brackets).

The parameters of the dedicated dynamic kalman filter (state vector including position, speed, drift, perturbation torque) have been tuned in order to reject the high frequency noise due to the controller.

These results give hopes for a 2-dimension random noise under 0.3 arcsec, i.e better than the specification all over the detector.

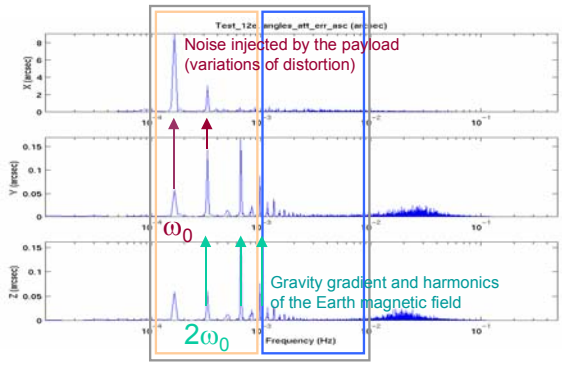

Fig. 16: Periodic perturbations due to the ACS.

We observe that the instrument harmonic errors at the orbital frequency ω_0 are not rejected. As expected, the spacecraft follows the small movements of the spots when the telescope is submitted to thermal variations. The gravity gradient is responsible for a line at $2\omega_0$ and the interaction of the spacecraft magnetic moment with the Earth magnetic field generates even harmonics up to 1 mHz. To sum up, despite several lines due to external environment in [0.1 ; 1] mHz, the polluted interval of frequencies is less than 40 μHz and the spectrum is perfectly clean in [1 ; 10] mHz. To better estimate the polluted interval of frequencies, the long term stability (coherence time) of the orbital perturbations should be assessed.

2.2.3. Focal unit and images

The focal plane is equipped with 4 E2V 4280 frame transfer CCD of 2048 x 2048 pixels, working in a Multi Pinned Phase (MPP) mode. This mode, associated with a temperature regulated at –40°C, reduces the dark currents to very low levels. The corresponding noise should be less than 1 electron/pixel/s rms. The 13.5 μm detectors are thinned, back illuminated, in order to have a high quantum efficiency (70% once integrated) in the bandwidth [370 nm ; 950 nm]. The images are 16 bits encoded.

This technology of detectors is used by ground observatories, but has not flown yet. A dedicated space evaluation has been undertaken by CNES. The best four CCD among ten manufactured have been selected at the Meudon observatory, according to criteria of well capacity and cartography of useless pixels.

The limited CCD well capacity (in MPP mode) and the jitter noise determine the size of the Point Spread Function (PSF) for the seismology channel. For a solar type star at the magnitude 5.7, the defocalized spot will be 410 pixels large.

Although two images per minute are enough for scientific data reduction, the ecartometric function asks the CCD to work at the higher rate of 1 image/s. The windowed readout is programmed by the video electronics.

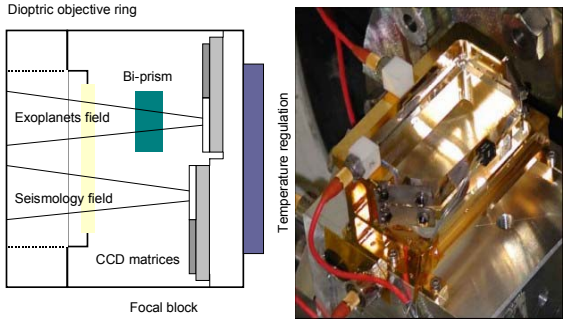

Fig. 17: Layout of the focal unit and picture of the prism (qualification model at IAS).

The exoplanet channel time exposure is 32 s. The spot size is about 80 pixels at the magnitude 13 for a K2 type star. For the faint stars of this field, the readout noise and the background are important contributors to the noise budget. The readout noise shall be limited to 5 electrons/pixel/s. Complete images are transmitted to the on-board extraction units in charge of soft windowing. It takes 22 s. The light dispersion (along the detector rows) is performed through the bi-prism inserted in front of the two exoplanets CCD.

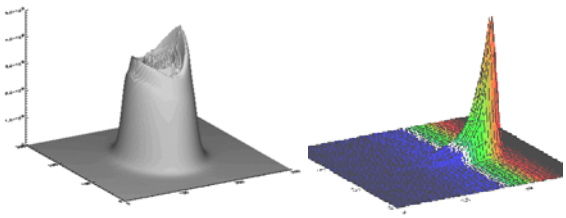

Fig.18: Examples of PSF for the seismology (left) and exoplanet (right) channels.

In order to correlate the photometric signal with external parameters like temperature or voltage, a series of calibrations is in the process of being done at different levels : CCD, camera, camera with readout electronics and complete photometric chain.

2.2.4. Thermal regulation

The thermal stability of the instrument will be carefully controlled in order not to introduce too high periodic fluctuations on the light curve induced by eclipses and orbital variations of terrestrial aspect. Thermal engineering, under CNES responsability with Soditech and Alcatel as contractors, follows an alveolar concept (5 alveoli: baffle, optics of the telescope, focal unit, upper and lower part of the equipment bay).

The telescope thermal architecture must provide a temperature stability in order not to exceed a variation of the star image bigger than 0.2 pixels on the orbital period (and 2 pixels on the long term). This has led to the choice of carbon-cyanate tubes, associated with a thermal control range of 20° ± 4° C. Multi Layer Insulators (MLI) surround the telescope structure.

Fig. 19: Mechanical part of the afocal (Alcatel): aluminum honeycomb sandwich plates, carbon truss, titanium insert for the camera, heater lines.

The instrument heating is realized by 11 platform-provided heater lines : 5 dedicated to the afocal, 2 for the dioptric objective and 4 for the equipment bay. Additional lines are provided at instrument level for fine tuning of the CCD and proximity electronics.

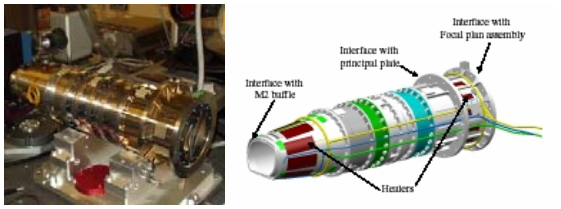

Fig. 20: Picture and CAD-view of the regulated dioptric objective (SODERN). Lens cylinders are made of titanium.

The equipment bay fine thermal regulation sub-system consists of (see Figure 21):

- Two aluminum heat distributors 15-30 mm thick, on which the video electronics and housekeeping electronics boxes are mounted.
- An aluminum heat distributor 4 mm thick for less sensible boxes (digitial units).
- Two heat distributor radiators, having a radiative surface of 400 x 100 mm^2.
- A set of thermistors and heaters.

MLI cover all the equipment bay, including every inner elementary component and Second Surface Mirror (SSM) sheets are used on the vertical sides and on the external face of the radiators.

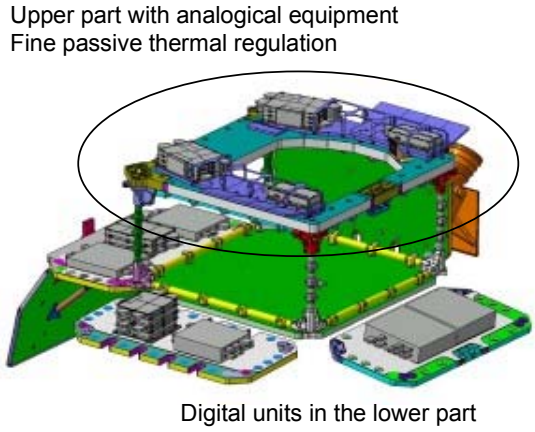

Fig. 21: Layout of the equipment bay (open).

The passive regulation of the equipment bay is compatible with two on-board photometric chains working continuously (stable heat dissipation). The price is a significant increase in mass : 25 kg.

Connected to a large radiator, with a surface of 940 x 280 mm^2 and oriented towards the instrument line of sight, the focal unit is at -40° C. This temperature is driven by active thermal regulation, necessary to achieve the stringent requirement of stability at CCD level : ± 0.015° C. A thermal sensor is fixed under the Invar block supporting the detectors.

As confirmed by the instrument CDR (Critical Design Review), the camera and the analogical electronics should have the following orbital variability:

Piece of equipment	Temperature variability	
Detector (CCD)	0.006° C	*(0.030° C)*
Dioptric objective (OD)	0.1° C	*(2.0° C)*
Proximity electronics (EP)	0.1° C	*(0.3° C)*
Video electronics (BCC)	0.15° C	*(0.3° C)*
Housekeeping (BS1)	0.8° C	*(2.0° C)*

Table 11: Peak-peak variability of equipment sensitive to temperature (specification between brackets).

This sound behavior has been demonstrated in many cases of simulation (to search the worst case). Nevertheless, the focal unit is expected to drive the mission due to the solar constraints on its radiator.

To filter the orbital variations and keep the CCD below -40° C (condition of the active regulation efficiency), a high temperature gradient is needed with the outside visible temperature. Despite a Flexible Solar Reflector (RSF) covering the Ys+ wall of the telescope to limit the infra-red flux toward the focal unit radiator, the outside temperature can increase as function of the roll angle (at the beginning or at the end of a half year period, when the direction of the Sun is lateral).

A set of pointing rules has been defined to help the users to optimize the stability of the instrument and to avoid bad geometrical configurations.

3. ON-BOARD TREATMENTS

The total scientific telemetry volume is 1.4 Gbits per day, received by a network of S band ground stations. Except for calibration operations, complete images cannot be downloaded : photometry is integrated on board within pre-defined masks.

3.1. Seismology channel

The on-board photometric chains are designed to process, for each CCD :

- 5 star windows (50x50 pixels^2) ;
- 5 sky reference windows (binning) ;
- 2 offset reference windows.

The aperture photometry (sum of the detected photons in all the pixels covered by the star image) is based on a maximal signal-to-noise criterion. A pixel belongs to the aperture (also called mask) if its average intensity is larger than the noise variance. Pixels belonging to another star inside the window are excluded from the set. This aperture will be the same for all images of a run and is not polluted by closeby faint stars as long as the two spots are not in contact.

The on-board software also corrects the photometry for a series of undesirable components: offset variations, dark currents and background variations, false pixels when crossing the South Atlantic Anomaly (high probability of proton events). The image of a star can be downloaded in 30x30 masks, if accumulated for 8 s at least.

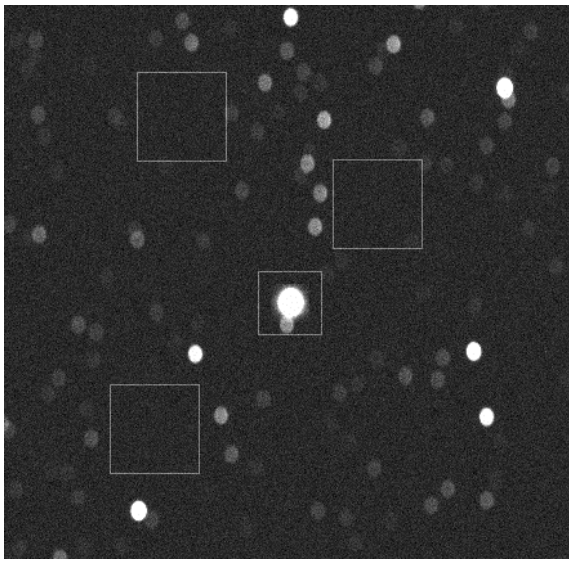

Fig. 22: Star and sky reference windows simulated around HD 43318 (image size : 15' x 15')

At least two stars of the seismology field are used for the ecartometry. The barycenter calculation is made using a threshold method.

3.2. Extrasolar planet channel

The exoplanet fields are characterized by a high density of objects up to the magnitude 23. The useful pixels represent only 10% of the CCD image.

The on-board photometric chains are designed to process, for each CCD :

- up to 5000 stars within chromatic masks ;
- 1000 stars within monochromatic masks ;
- 20 small sky reference images (10x15 pixels^2) ;
- 32 offset reference windows.

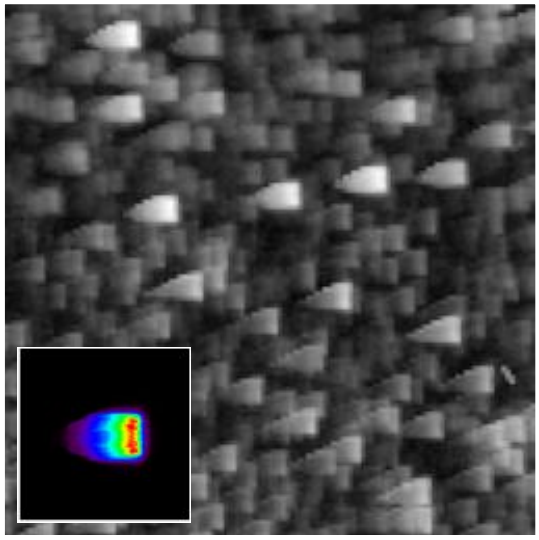

Fig. 23: Simulated exoplanet field up to mv=18 and example of a three color spectrum (inlay).

The masks have to be programmed among a pre-defined list of uploaded patterns. The monochromatic masks are used for faint and cold stars analyzed in white light, as well as for background references.

The shape of the mask is a function of several parameters:

- the magnitude of the star,
- the temperature of the star (or its color),
- the local shape of the PSF on the CCD,
- the contamination of the target by closeby stars.

It has been shown by simulation that 256 different patterns allow the fitting of every possible target. A system tool has been developped to determine the optimal programming of an exoplanet observing run, taking into account the mask definition criteria, the behavior of the instrument (PSF variations, local noise or CCD defaults) and a number of effects such as spot overlapping and smearing.

The on-board software calculates the photometry in one or three colors, as requested by telecommand, and accumulates the data during 16 exposures (8.5 minutes). The movements of the line of sight make the image spot move on the surface of the CCD and the dispersed colors blend together over the mask. It has been demonstrated that a correction of this depointing noise is possible on ground. This correction consists in interpolating the three color light curves obtained for each chromatic mask, using a reference spectrum (downloaded in a preliminary calibration phase) and the attitude data coming from the seismology channel. This approach makes the implementation of the on-board software easier.

Up to 500 stars can be oversampled to 32 s, in case a transit event is expected after a first alarm. Every other correction of the light curve will be done on the ground.

Conclusion

The COROT experiment addresses major scientific topics. Designed to study the internal structure of many families of stars, it has been adapted to the detection of planetary transits (same interest in long continuous runs and in accurate photometry). The discovery of terrestrial planets by COROT is the next challenge after the harvest of Jupiter-like objects. Besides, the COROT stellar microvariability database, containing the light curves of thousands of stellar objects, will provide the astronomical community with wide research opportunities.

The project activity is currently focused on the instrument manufacturing and testing. Straylight rejection in low earth orbit, pointing, thermal stability and photometry processing are the main critical points of the mission, for which cost-effective compromises have been found. The system Preliminary Design Review was held in October 2003 and the Critical Design Review of the instrument has just authorized the integration phase for a delivery of the flight model in 2005. The launch is scheduled in the summer of 2006 by a SOYUZ/ST launcher from Baïkonour.

Project Team

The mission is led by CNES and the following French laboratories:

- Observatoire de Paris (Laboratoire d'Etudes Spatiales et d'Instrumentation en Astrophysique), involved in the development of the camera, the on-board software, the equipment bay and the ground data processing for seismology ;
- Laboratoire d'Astrophysique de Marseille, in charge of the telescope and the ground data processing for exoplanets ;
- Institut d'Astrophysique Spatiale (Orsay), in charge of the camera calibrations and the prism manufacturing ;
- Observatoire Midi-Pyrénées (Toulouse), which builds the catalogues to prepare the runs.

The scientific committee, with members of the seven partners, is led by Annie Baglin, PI.

Cooperation

The European partners of COROT, contributing to the development of the instrument, are: Austria, Belgium, ESA, Germany and RSSD (ESTEC). Spain and Brazil contribute to the ground segment (software for the mission center and earth terminal in Natal).

References

(1) L. Boisnard, M. Auvergne: *COROT system requirements for accurate stellar photometry.* IAF 2001, 52nd International Astronautical Congress.
(2) T. Viard, P. Bodin, A. Magnan: *COROT Telescope development.* ICSO 2004, 5th Conference.

Contact

For more information and links towards other sites, one can contact the internet server:
http://corot-mission.cnes.fr

Acknowledgements

The content of this paper represents the work of the COROT project team, gathering people working at CNES as well as in many laboratories. We want to give credit to their skill and their contribution. Special thanks to Annie Baglin, Pierre Bodin, Tristan Buey, Vincent Costes, Gerard Epstein, Philippe Gamet, Hervé Hustaix, Christian Imbert, Martine Jouret, Thien Lam-Trong, Patrick Levacher, Alain Magnan, Marc Ollivier, Philippe Plasson, Didier Tiphène.